View metadata, citation and similar papers at core.ac.uk

brought to you by CORE

provided by Caltech Authors

PROCEEDINGS OF SPIE

SPIEDigitalLibrary.org/conference-proceedings-of-spie

Scaling multiconjugate adaptive optics performance estimates to extremely large telescopes

Brent L. Ellerbroek, Francois J. Rigaut

Brent L. Ellerbroek, Francois J. Rigaut, "Scaling multiconjugate adaptive optics performance estimates to extremely large telescopes," Proc. SPIE 4007, Adaptive Optical Systems Technology, (7 July 2000); doi: 10.1117/12.390314

SPIE.

Event: Astronomical Telescopes and Instrumentation, 2000, Munich, Germany

Downloaded From: https://www.spiedigitallibrary.org/conference-proceedings-of-spie on 6/29/2018 Terms of Use: https://www.spiedigitallibrary.org/terms-of-use

Scaling Multi-Conjugate Adaptive Optics Performance Estimates to Extremely Large Telescopes

B.L. Ellerbroek and F.J. Rigaut[1]

Gemini Observatory
670 N. A'ohoku Place
Hilo, Hawaii 96720

ABSTRACT

Multi-conjugate adaptive optics (MCAO) is a key technology for extremely large, ground-based telescopes (ELT's) because it enables near-uniform atmospheric turbulence compensation over fields-of-view considerably larger than can be corrected with more conventional AO systems. Quantitative performance evaluation using detailed analytical or simulation models is difficult, however, due to the very large number of deformable mirror (DM) actuators, wave front sensor (WFS) subapertures, and guide stars which might comprise an MCAO system for an ELT. This paper employs more restricted minimal variance estimation methods to evaluate the fundamental performance limits imposed by anisoplanatism alone upon MCAO performance for a range of sample cases. Each case is defined by a atmospheric turbulence profile, telescope aperture diameter, field-of-view, guide star constellation, and set of DM conjugate ranges. For a Kolmogorov turbulence spectrum with an infinite outer scale, MCAO performance for a whole range of aperture diameters and proportional fields-of-view can be computed at once using a scaling law analogous to the $(D/d_0)^{5/3}$ formula for the cone effect. For 30 meter telescopes, useful levels of performance are possible across a 1.0–2.0 arc minute square field-of-view using 5 laser guide stars (LGS's) and 3 DM's, and somewhat larger fields can be corrected using 9 guide stars and 4 mirrors. 3 or more tip/tilt natural guide stars (NGS's) are necessary to detect modes of tilt anisoplanatism which cannot be detected using LGS's, however. LGS MCAO performance is a quite weak function of aperture diameter for a fixed field-of-view, and it is tempting to scale these results to larger apertures. NGS MCAO performance is moderately superior to LGS MCAO if the NGS constellation is within the compensated field-of-view, but degrades rapidly as the guide stars move away from the field. The penalty relaxes slowly with increasing aperture diameter, but how to extrapolate this trend to telescopes with diameters much larger than 30 meters is unclear.

Keywords: Multi-conjugate adaptive optics, extremely large telescopes

1 INTRODUCTION

Multi-conjugate adaptive optics (MCAO) is a proposed approach for compensating atmospheric turbulence across extended fields-of-view which are much larger than can be corrected using conventional adaptive optics. MCAO employs deformable mirrors (DM's) at several conjugate ranges, which are commanded to null the wave front sensor (WFS) measurements from guide stars in several different directions. The concept was apparently first proposed in 1989 [1], evaluated quantitatively for sample scenarios in 1994 [2, 3], and has more recently been the subject of simulation and analysis for 4 to 8 meter telescopes [4, 5]. Encouraging results have also been obtained in a test of tomographic wave front sensing involving multiple natural guide stars (NGS's) [6]. MCAO is now proposed almost routinely for the 30 to 100 meter class telescopes presently under discussion [7] However, quantitative MCAO performance analysis for such extremely large telescopes (ELT's) is difficult due to the very large number of DM

[1]Further author information –
BLE: Email: bellerbroek@gemini.edu; Telephone: (808) 974-2575; Fax: (808) 935-9235
FJR: Email: frigaut@gemini.edu; Telephone: (808) 974-2505; Fax: (808) 935-9235

In *Adaptive Optical Systems Technology*, Peter L. Wizinowich, Editor,
Proceedings of SPIE Vol. 4007 (2000) • 0277-786X/00/$15.00

Downloaded From: https://www.spiedigitallibrary.org/conference-proceedings-of-spie on 6/29/2018
Terms of Use: https://www.spiedigitallibrary.org/terms-of-use

actuators and WFS subapertures involved, as well has the high dimensionality of the tradespace for performance optimization. Current analytical techniques and simulation programs for detailed evaluation of AO systems on smaller telescopes break down due to the computer requirements, which scale as the sixth power of the aperture diameter. Substantial improvements in computational algorithms and efficiency will be necessary for comprehensive mathematical modeling of AO for ELT's. Fortunately, it is still possible obtain partial solutions to this problem using simpler methods.

This paper summarizes some preliminary results on this topic. Anisoplanatism will remain an important source of wave front error for MCAO systems, since a finite number of WFS's and DM's will never be able to entirely compensate for the effects of a continous atmosphere. Understanding how the number and configuation of DM's, WFS's, and their associated guide stars determine this fundamental limit on MCAO performance is an important early step in developing system specifications for an ELT. By neglecting all other sources of wavefront error–WFS noise, DM/WFS fitting error, time delay, static and dynamic telescope errors–the computation requirements to analytically evaluate the mean-square, aperture- and field-averaged phase distortion due to anisoplanatism can be reduced to a level where trade studies of potential system performance become feasible.

For an idealized minimal variance wave front reconstruction algorithm derived from atmospheric turbulence statistics and the configuation of DM's and guide stars, the residual phase variance σ^2 due to anisoplanatism is a function of (i) the turbulence power spectrum, (ii) the atmospheric refractive index structure constant $C_n^2(z)$, (iii) the telescope diameter D, (iv) the vector of angles $\vec{\theta}$ describing the guide stars locations and the performance evaluation directions, and (v) the vector $\vec{h}$ of DM conjugate altitudes. For MCAO systems based upon laser guide stars (LGS's) the vector $\vec{\theta}$ must be augmented to include the directions of the one or more natural guide stars (NGS's) used for tip/tilt or possibly low-order wave front sensing, and the vector $\vec{h}$ must also include the guide star altitudes. In the special case of a Kolmogorov spectrum with an infinite outer scale, the relationship between the phase variance σ^2 and these parameters can be described by the scaling law of the form

$$\sigma^2 = (D/r_0)^{5/3} f(C_n^2, \vec{h}, \vec{\theta}/D). \tag{1}$$

This is analogous to the formula $\sigma^2 = (D/d_0)^{5/3}$ the cone effect, where the parameter d_0 is function of C_n^2 and a single guide star altitude h. The function f must be computed numerically from very large matrices with elements defined as integrals involving the function $C_n^2(z)$ and the guide star/DM configuation, but only a single evaluation is required for the entire one-dimensional family of configuations with the given value of $\vec{\theta}/D$. MCAO performance for a 20 meter aperture diameter and 1 arc minute field of view can be evaluated at the same time as for a 40 meter system with a 2 arc minute field of view, *provided that the directions of all natural- and laser guide stars also scale up proportionately.*

Section 2 briefly sketches a derivation leading up to this scaling law. The approach taken is similar to many previous developments of minimal variance wave front reconstruction algorithms, some of which have considered a wider range of AO error sources beyond anisoplanatism [8, 9, 10, 2, 3]. Section 3 outlines sample results obtained for representative Mauna Kea (MK) and Cerro Pachon (CP) turbulence profiles, and MCAO configurations with 3 or 4 deformable mirrors, 5 or 9 natural- or laser guide stars, and square fields of view. The LGS MCAO systems also utilize 1 or 4 natural guide stars for either tip/tilt sensing or low order wave front sensing. The performance estimates for the CP are very similar to MK; the isoplanatic angle θ_0 is somewhat larger for the former site, and the smaller value of r_0 is not a handicap because fitting error is not included in the analysis. For either site, an MCAO system with 5 guide stars and 4 DM's achieves a level of performance which would be useful for observations at 2.2 microns with a 30 meter telescope over about a 1.5 arc minute field of view. Roughly similar results are obtained with natural- and laser guide stars, although (i) the LGS MCAO system requires multiple tip/tilt natural guide stars to detect certain atmospheric modes producing tilt anisoplanatism, and (ii) performance with NGS MCAO degrades very rapidly as the locations of the guide stars move away from the desired field-of-view. This penalty decreases slowly with increasing aperture diameter, but we are not able to quantitatively extrapolate this trend to 100 meters at this time.

Downloaded From: https://www.spiedigitallibrary.org/conference-proceedings-of-spie on 6/29/2018
Terms of Use: https://www.spiedigitallibrary.org/terms-of-use

2 SUMMARY OF ANALYSIS

The approach used in this paper to evaluate MCAO performance for the special case of geometrical optics has been described previously in several earlier papers on MCAO and LGS AO performance [9, 2]. As used here the method is restricted to evaluating the wavefront correction error due to anisoplanatism with a finite number of guide stars and deformable mirrors, and does not consider other error sources such as WFS noise, WFS/DM fitting error, time delay, and noncommon path aberrations. Analytical methods and software do exist to provide an integrated treatment of these effects [3, 11], but for now they are restricted to systems with on the order of 1000 DM actuators and WFS subapertures on account of computation requirements. This section sketches the simplified approach used here in enough detail to justify the form of the scaling law given in Eq. (1) above.

The purpose of the MCAO system is to derive a vector of DM actuator commands a based upon a WFS measurement vector y, in order to compensate for a vector turbulence-induced phase distortion values x. For MCAO all three of these vectors include components associated with the multiple DM's, WFS's, and evaluation directions in the science field. The phase vector x has the piston component (or average value) of the phase for each evalutation direction subtracted off. The DM commands a are determined from the WFS measurements y by an equation of the form

$$a = Ey, \tag{2}$$

where E is the reconstruction matrix. The mean-square phase error after applying the correction is given by

$$\sigma^2 = \frac{1}{N_e N_p} ||x - Ha||^2, \tag{3}$$

where N_e is the number of evaluation directions, N_p is number of points sampled in the telescope aperture, and H is the influence function matrix from DM actuator commands to phases in each of the evaluation directions. The matrix E must be optimized to evaluate MCAO performance for each system configuation and set of atmospheric conditions. The optimized phase variance and the corresponding reconstruction matrix are defined as

$$\sigma_*^2 = \min_E \langle \sigma^2 \rangle , \tag{4}$$

$$E_* = \arg\min_E \langle \sigma^2 \rangle , \tag{5}$$

where the angle brackets, $\langle \cdots \rangle$, denote ensemble averaging over atmospheric turbulence statistics.

By writing the norm of the vector in Eq. (3) as an inner product and substituting Eq. (2) for a, the expected value of σ^2 is given by

$$\begin{aligned} \langle \sigma^2 \rangle &= \frac{1}{N_e N_p} \langle (x - HEy)^T (x - HEy) \rangle \\ &= \frac{1}{N_e N_p} \langle \mathrm{tr} \left[(x - HEy)(x - HEy)^T \right] \rangle . \end{aligned} \tag{6}$$

Here the superscript T denotes the transpose of a matrix or vector, and $\mathrm{tr}(M)$ is the trace of a square matrix M. Distributing the vector outer product and using the fact that H and E are nonrandom enables Eq. (6) to be rearranged into the form

$$\langle \sigma^2 \rangle = \frac{1}{N_e N_p} \mathrm{tr} \left(A - HEB^T - BE^T H^T + HECE^T H^T \right) , \tag{7}$$

where A, B, and C are used to represent the covariance matrices

$$A = \langle xx^T \rangle , \tag{8}$$

$$B = \langle xy^T \rangle , \tag{9}$$

$$C = \langle yy^T \rangle . \tag{10}$$

Downloaded From: https://www.spiedigitallibrary.org/conference-proceedings-of-spie on 6/29/2018
Terms of Use: https://www.spiedigitallibrary.org/terms-of-use

Eq. (7) for $\langle \sigma^2 \rangle$ is quadratic in the coefficients of E, and the global minimum may be found by setting all partial derivatives equal to zero. The result is given by the usual expressions

$$E_* = (H^T H)^\dagger H^T B C^\dagger, \tag{11}$$

$$\sigma_*^2 = \frac{1}{N_e N_p} \mathrm{tr}\left[A - (H^T H)^\dagger (H^T B) C^\dagger (H^T B)^T\right], \tag{12}$$

where $M^\dagger$ is the pseudo-inverse of a square matrix M.

It remains to evaluate the covariance matrices A, B, and C. To do so, the vectors x and y of phase distortions and WFS measurements must be described in greater detail. The vector x takes the form

$$x = \begin{pmatrix} T_1 \phi_1 \\ \vdots \\ T_N \phi_N \end{pmatrix}, \tag{13}$$

where ϕ_i is the turbulence-induced phase profile for evaluation direction number i sampled on a discrete grid of aperture points, and T_i is a matrix which removes the average value from the phase profile. Similarly, y, is described by the expression

$$y = \begin{pmatrix} T_{N+1} \phi_{N+1} \\ \vdots \\ T_{N+M} \phi_{N+M} \end{pmatrix}, \tag{14}$$

where ϕ_{N+j} is the phase profile for guide star number j sampled at a discrete grid of aperture points, and the matrix T_{N+j} transforms these phase values into WFS measurements. For a Shack-Hartmann WFS, for example, each row of T_{N+j} represents a line integral along the boundary of a WFS subaperture [8], and full-aperture tilt removal for laser guide stars can be implemented by an additional matrix multiply. It follows from the above that each of the covariance matrices A, B, and C consist of blocks of the form $T_i \langle \phi_i \phi_j^T \rangle T_j^T$. In what follows we focus on the calculation of the covariance $\langle \phi_i(x) \phi_j(x') \rangle$ for two points x and x' in the aperture plane, since this is sufficient to demonstrate the scaling law given in Eq. (2).

Neglecting the effects of scintillation and diffraction, the turbulence-induced phase distortion experienced by the light propagating from evaluation direction or guide star number i is described by the equation

$$\phi_i(x) = k \int_0^Z dz\, n\left[\left(1 - \tfrac{z}{z_i}\right) x + z\theta_i, z\right]. \tag{15}$$

Here $k = 2\pi/\lambda$ is the wavenumber for the wavelength λ, Z is the lesser of the range to the guide star or edge of the atmospheric, z is the variable of integration for the paraxial ray path between the point x in the aperture to the guide star, $n(r, z)$ is the refractive index variation due to turbulence at range z and transverse coordinates r, z_i is the range to the guide star, and θ_i is the direction to the guide star from the origin of the telescope aperture. The phase covariance $\langle \phi_i(x) \phi_j(x') \rangle$ can be rewritten in the form

$$\langle \phi_i(x) \phi_j(x') \rangle = \langle \phi_i^2(x) \rangle + \langle \phi_j^2(x') \rangle - \tfrac{1}{2} \left\langle [\phi_i(x) - \phi_j(x')]^2 \right\rangle. \tag{16}$$

Only the last of the three terms on the right-hand-side need be evaluated, since the first two terms are actually independent of x and x', and each of the possible values of T_i in Eq.'s (13) and (14) will null single-valued vectors. For a Kolmogorov turbulence spectrum with an infinite outer scale, the mean-square phase difference in Eq. (16) has the value

$$\left\langle [\phi_i(x) - \phi_j(x')]^2 \right\rangle = \left(\frac{6.88}{r_0^{5/3}}\right) \frac{\int dz\, C_n^2(z) \left| \left(1 - \frac{z}{z_i}\right) x - \left(1 - \frac{z}{z_j}\right) x' + z(\theta_i - \theta_j) \right|^{5/3}}{\int dz\, C_n^2(z)}, \tag{17}$$

Downloaded From: https://www.spiedigitallibrary.org/conference-proceedings-of-spie on 6/29/2018
Terms of Use: https://www.spiedigitallibrary.org/terms-of-use

where r_0 is the turbulence-induced effective coherence diameter at the wavelength λ, and $C_n^2(z)$ is the refractive index structure constant at range z. This last result can be rearranged slightly into the form

$$\left\langle [\phi_i(x) - \phi_j(x')]^2 \right\rangle = 6.88 \left(\frac{D}{r_0}\right)^{5/3} \int dz\, c(z) \left| \left(1 - \frac{z}{z_i}\right) \frac{x}{D} - \left(1 - \frac{z}{z_j}\right) \frac{x'}{D} + z\left(\frac{\theta_i}{D} - \frac{\theta_j}{D}\right) \right|^{5/3}, \tag{18}$$

where D is the telescope aperture diameter, and the function $c(z)$ is an abbreviation for the normalized C_n^2 profile given by

$$c(z) = \frac{C_n^2(z)}{\int dz\, C_n^2(z)}. \tag{19}$$

We now finally consider how the results of these calculations will vary with telescope diameter D with all other parameters fixed. The mean-square phase difference in Eq. (18) will scale as $(D/r_0)^{5/3}$ provided that (i) the ratios x/D and x'/D are constant (i.e., the coordinates of the grids of points used to sample the phase profiles ϕ_i scale with D), and (ii) the ratios θ_i/D are also constant. The matrices T_i and the DM-to-phase influence matrix H appearing in Eq.'s (12) through (14) are also constant given these assumptions. It follows that the covariance matrices A, B, and C, and also the minimized mean-square phase variance σ_*^2, all scale with $(D/r_0)^{5/3}$ as summarized by Eq. (1). A single numerical calculation can therefore be used to evaluate a MCAO performance for an entire one-dimensional family of telescope diameters and fields-of-view, at least for the case of an infinite outer scale.

3 NUMERICAL RESULTS

This section presents numerical results on MCAO performance for sample atmospheric turbulence profiles and several representative natural- and laser guide star configurations. Table 1 lists the two turbulence profiles considered, which are discrete fits to median $C_n^2(h)$ measurements at Mauna Kea [12] and Cerro Pachon [13]. The field-of-view and guide star geometries evaluated are illustrated in Fig. 1. All of the results in this section are for square fields-of-view, with MCAO performance averaged over the nine points illustrated in Fig. 1a. The half-width of the field-of-view is denoted θ. Fig.'s 1b and 1c illustrate the constellations of 5 and 9 guidestars considered for higher-order wave front sensing. The half-width of these square constellations is denoted θ_B, with the variable $r = \theta_B/\theta$ representing the ratio of these two angles. Intuition and a few sample results presented below suggest that $r = 1$ should be close to optimal for minimizing the residual phase variance, and this value has been used for the most of the LGS MCAO calculations presented in this section. For natural guide stars we have considered $r = 1$ and 2, but we are unclear on the correct value to use based upon guide star density considerations.

As with current LGS AO systems, LGS MCAO systems must also incorporates at least one low-order NGS WFS to measure the tip/tilt wave front errors which are (at least presently) unmeasurable using a LGS. One NGS is sufficient to measure tip/tilt for a single direction, but at least three are required to measure tilt anisoplanatism effects across an extended field-of-view. In this section we consider the constellation of 4 tip/tilt NGS illustrated in Fig. 1d, which reduces computation requirements by reason of symmetry. Low-order (LO) natural guide star wave front sensing with from 2×2 to 5×5 subapertures has also been considered, since this "hybrid" guide star approach has been found to help compensate for the cone effect in some previous calculations.

All calculations with 5 higher-order guide stars have also assumed 3 deformable mirrors conjugate to altitudes of 0, 4, and 8 kilometers. The constellation of 9 guide stars has been paired with 4 DM's conjugate to 0, 2.67, 5.33, and 8.0 kilometers.

As described in section 2 these calculations discretize the telescope aperture into a set of points on an $N \times N$ grid, where $8 \leq N \leq 20$. Higher-order WFS measurements are modelled as phase differences between adjacent grid points, with full-aperture averages subtracted from the LGS measurements. Low-order NGS measurements are modelled as the average $x-$ and y phase differences within square subapertures. DM phase adjustments are discretized using the

Downloaded From: https://www.spiedigitallibrary.org/conference-proceedings-of-spie on 6/29/2018
Terms of Use: https://www.spiedigitallibrary.org/terms-of-use

Layer	Cerro Pachon		Mauna Kea	
	h, meters	Fractional C_n^2	h, meters	Fractional C_n^2
1	0	0.646	90	0.003
2	1800	0.078	1826	0.136
3	3300	0.119	2720	0.163
4	5800	0.035	4256	0.161
5	7400	0.025	6269	0.167
6	13100	0.080	8340	0.235
7	15800	0.015	10546	0.068
8			12375	0.032
9			14610	0.023
10			16471	0.006
11			17028	0.007

Table 1: $C_n^2(h)$ profiles for MCAO calculations

These two profiles are discretized fits to median $C_n^2(h)$ measurements at Cerro Pachon and Mauna Kea. h is the altititude above the site. The values of r_0 for the two profiles are 0.166 (CP) and 0.236 (MK) meters at 0.5 microns. The values of θ_0 are 2.74 and 2.29 arc seconds.

same grid. To avoid interpolating the phase adjustments, we require that $N\theta h/D$ be an integer for each deformable mirror altitude h, so that rays traced from the array of aperture grid points in any of the nine evaluation directions will also pass through the array of grid points at each DM altitude.

To evaluate MCAO performance for a fixed field size θ and a range of aperture diameters D, N varies proportionately with D so that the grid spacing remains fixed. This guarantees that the same spatial scales of turbulence are considered for all diameters, and that smaller telescopes are not penalized by including turbulence effects on a smaller scale. The calculations using 8 grid points are intended to represent an 8 meter telescope with a half field-of-view θ given by $8 \cdot \theta \cdot 4000/8 = 1$, so that $\theta = 250\,\mu\text{rad} = 51.5\,\text{arc sec}$. This is the most coarsely discritized calculation presented in this section, and we have checked that the computed phase variances are reasonable approximations to the values computed using more detailed models.

Finally, the subaperture width d_{SA} for the low-order NGS WFS's is defined by $Nd_{SA}/D = 4$, so that the width of the subaperture is fixed at 4 grid points. As N increases from 8 to 20, the number of subapertures across the LO NGS WFS increases from 2 to 5. Since N is proportional D for fixed θ, the physical width of the subapertures is independent of D.

Separately optimizing the guide star geometry on a case-by-case basis would be very computationally intensive, and intuition suggests that a value $r = 1$ for the ratio between the widths of the science field and the guide star constellation should be at least reasonable. Fig. 2 plots the normalized residual phase variance $\sigma^2/(D/r_0)^{5/3}$ as a function of r for one particular set of atmospheric and AO system parameters as described in the caption. The normalized phase variance at $r = 1$ is reasonably near the minimum. This value has been used for the rest of LGS MCAO calcuations in this section, since the goal here is to study trends and compare options rather than fully optimize a small set of results.

Fig. 3 plots the normalized phase variance $\sigma^2/(D/r_0)^{5/3}$ as a function of the normalized beam shear $h\theta/D$ with $h = 8000\,\text{m}$, the range of the furthest deformable mirror. These results are for the turbulence profile derived from median Cerro Pachon measurements, but the results for the Mauna Kea profile are qualitatively very similar. Results are plotted for six MCAO configurations, each with 5 higher order guide stars:

Downloaded From: https://www.spiedigitallibrary.org/conference-proceedings-of-spie on 6/29/2018
Terms of Use: https://www.spiedigitallibrary.org/terms-of-use

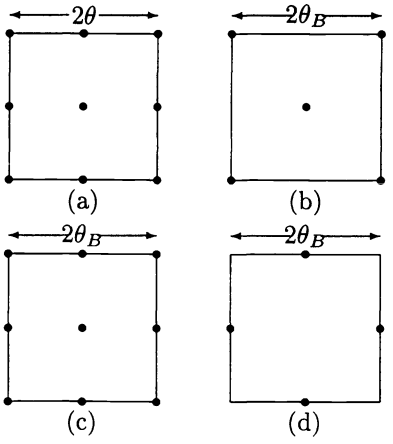

Figure 1: Science field and guide star configurations for MCAO calculations

These schematics illustrate the arrays of directions used for MCAO performance evaluation (a), higher-order guide stars (b and c), and tip/tilt or low-order NGS WFS's with LGS MCAO (d).

- LGS systems with 1 tip/tilt NGS, 4 tip/tilt NGS's, or 4 LO NGS's;
- NGS systems with $r = 1$, 2, or 3.

The normalized phase variance improves with decreasing $h\theta/D$ for all six options. If θ is decreasing with D fixed, this improvement translates directly into smaller phase variances and higher Strehl ratios. If θ is fixed and D is increasing, the improvement is contradicted by the increasing value of $(D/r_0)^{5/3}$, and that the extent of the actual improvement (or lack of it) depends upon the slope of the curves plotted in Fig. 3.

Not surprisingly, the best results are achieved for the NGS MCAO system with $r = 1$. The performance curves for the three LGS cases are very nearly parallel to this first case, so that the ratios of the residual phase variances between these cases is very nearly independent of $h\theta/D$. For LGS MCAO with 4 low-order (LO) NGS WFS the ratio is about 1.25:1, so the observing wavelength must be increased by a factor $1.25^{1/2} = 1.12$ for equal performance in terms of the residual phase variance, and the Strehl ratio at the same wavelength (due anisoplanatic effects only) is reduced by exponentiation to the power 1.25. For LGS MCAO with 4 tip/tilt guide stars the ratio is somewhat poorer at 1.55:1, while with only 1 tip/tilt guide star it is considerably worse at about 4:1. This last result can be explained by the fact that tilt anisoplanatism cannot be measured using a single tip/tilt NGS and *any* number of tilt-removed guide stars at a single range.

The performance of the NGS MCAO options for different values of r is not described by simple constants of proportionality. Increasing r to 2 or 3 increases the normalized phase variance by a larger factor when the normalized beam shear is large. For a normalized beam shear of 0.23 at the edge of the science field, $r = 2$ or 3 increases the shear to a value of 0.46 or 0.69 for the guide stars, and the accuracy of wave front tomography is significantly degraded. For a normalized beam shear of 0.10 for the science field, the corresponding beam shears for the guide stars is increased to only 0.2 or 0.3, and the performance penalty is somewhat less significant. We cannot quantitatively predict how this trend will continue as the normalized beam shear decreases further.

Fig. 4 presents analogous results for MCAO systems with 9 higher-order guide stars and 4 deformable mirrors. The

Downloaded From: https://www.spiedigitallibrary.org/conference-proceedings-of-spie on 6/29/2018
Terms of Use: https://www.spiedigitallibrary.org/terms-of-use

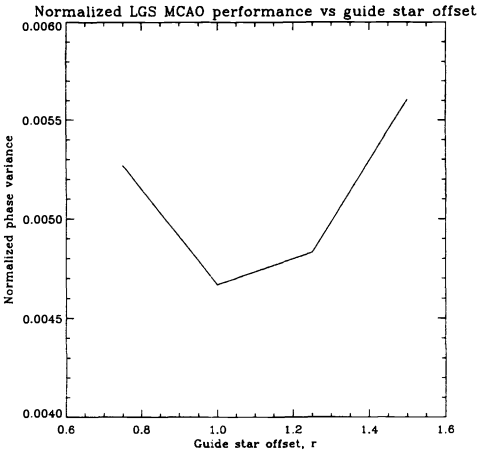

Figure 2: Sample LGS MCAO performance vs guide star offset

These results are for an LGS AO system with 5 higher-order guide stars, 4 low-order NGS WFS with 4×4 subapertures, 3 DM's conjugate to ranges of 0, 4, and 8 km, and the Cerro Pachon turbulence profile. The normalized size of the science field θ is given by $8000 \cdot \theta/D{=}1/8$, where D is the telescope diameter in meters. This sample case illustrates that, as might be expected, matching the guide star constellation to the size of the of the science field ($r = 1$) results in near-optimal MCAO performance.

trends are qualitatively very similar, as are the results computed for the Mauna Kea turbulenc profile. Comparing Fig's. 3 and 4 at a beam shear of 0.2, the performance of the best NGS and LGS options has improved by factors of slightly more than 3 and 2, respectively, due to the increase in the numbers of DM's and guide stars.

Fig. 5 interprets the normalized results in Fig.'s 3 and 4 for quantitative aperture diameters and field-of-view. For each field-of-view considered (1, 1.5, 2, and 3 arc minutes full width), the normalized beam shears considered in Fig.'s 3 and 4 correspond to a different range of aperture diameters, which increases proportionately with θ. Once D is specified, the normalized phase variances can be converted to an RMS optical path difference (OPD).[2] To avoid clutter, results have been plotted for only three MCAO configuations:

- NGS MCAO with $r = 1$ and 2,
- LGS MCAO with low-order NGS WFS's.

NGS MCAO with $r = 1$ and LGS MCAO produce roughly comparible results for the three DM cases, while NGS MCAO with $r = 2$ is appreciably worse. The RMS OPD for the first two cases is in the range 0.10–0.12 microns for $D = 12\,\text{m}$ and $2\theta = 1\,\text{arc min}$, 0.14–0.16 microns for $D = 20\,\text{m}$ and $2\theta = 1.5\,\text{arc min}$, and 0.19–0.21 microns for $D = 30\,\text{m}$ and $2\theta = 2.0\,\text{arc min}$. These are useful levels of atmospheric turbulence compensation in K band (2.2 microns), and even at shorter wavelengths for the two smaller fields of view. The performance variations with D are so slight for these two MCAO configurations that it is very tempting to extrapolate these results to larger values of D, but further calcuations are certainly desirable.

The performance of the third MCAO configuation considered, NGS MCAO with $r = 2$, improves with increasing aperture diameter. It is not clear from the results in Fig. 5 how this trend will continue with increasing D, or what

[2]This RMS OPD is the wave front error due to anisoplanatism, and does not include the effects of WFS noise, WFS/DM fitting error, or servo lag.

Downloaded From: https://www.spiedigitallibrary.org/conference-proceedings-of-spie on 6/29/2018
Terms of Use: https://www.spiedigitallibrary.org/terms-of-use

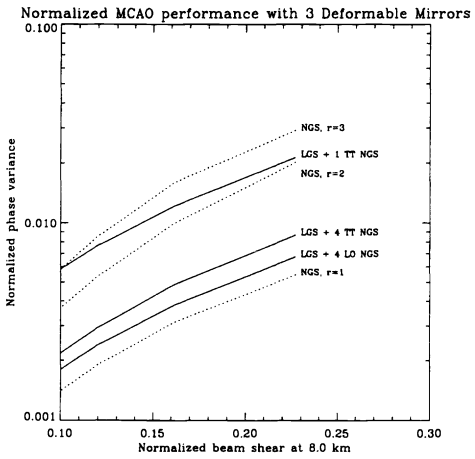

Figure 3: Normalized MCAO performance with 3 deformable mirrors

These results are for the median Cerro Pachon turbulence profile listed in Table 1. Fig. 1 illustrates the guidestar geometries (all with 5 higher order guide stars) for the six AO configuations considered. The normalized shear is the quantity $\theta \cdot h/D$, where θ is the half-width of the compensated field of view, $h = 8000\,\mathrm{m}$ is the conjugate altitude of the final deformable mirror, and D is the telescope aperture diameter in meters. The normalized phase variance is $\sigma^2/(D/r_0)^{5/3}$, where σ^2 is the mean-square phase error averaged over 9 points in the compensated field-of-view as illustrated in Fig. 1, and r_0 is the turbulence-induced effective coherence diameter.

value of r should be used based upon sky coverage and guide star density considerations. Futher work using more sophisticated analytical and/or computational techniques will be required to resolve these questions.

The bottom part of Fig. 5 plots results for MCAO configuations with 4 DM's and 9 higher-order guide stars. The improvement in performance is nonnegligible, but these results are less constant and harder to extrapolate with high confidence.

Finally, Fig. 6 plots the analogous results for the Mauna Kea turbulence profile. The results are very similar, which probably could not have been predicted in advance based upon the values of r_0 and θ_0 for the two profiles. MCAO performance is a function of the higher moments of the $C_n^2(h)$ turbulence profiles, and predicting MCAO performance for a specific profile may not be possible without significant computation.

Acknowledgements

The Gemini 8-m Telescopes Project and Observatory is managed by the Association of Universities for Research in Astronomy, for the National Science Foundation and the Gemini Board, under an international partnership agreement.

REFERENCES

[1] J.M. Beckers, "Detailed Compensation of Atmospheric Seeing using Multi-Conjugate Adaptive Optics," *SPIE* **1114**, 215–217 (1989).

Downloaded From: https://www.spiedigitallibrary.org/conference-proceedings-of-spie on 6/29/2018
Terms of Use: https://www.spiedigitallibrary.org/terms-of-use

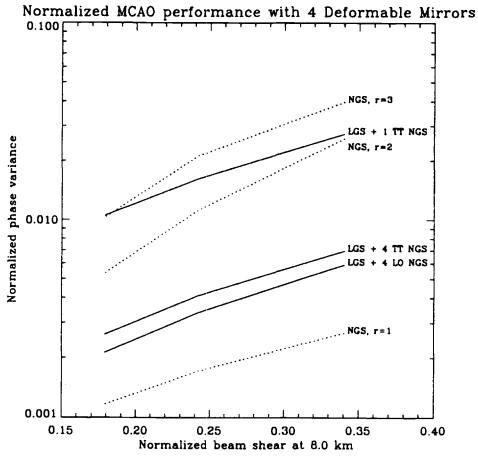

Figure 4: Normalized MCAO performance with 4 deformable mirrors

This figure is analogous to Fig. 3, except that the MCAO system configurations include four deformable mirrors and 9 higher-order guide stars. The altitude of the highest deformable mirror is still 8000 m.

[2] D.C. Johnston and B.M. Welsh, "Analysis of multiconjugate adaptive optics," *J. Opt. Soc. Am. A* **11**, 394–408 (1994).

[3] B.L. Ellerbroek, "First-order performance evaluation of adaptive-optics systems for atmospheric-turbulence compensation in extended-field-of-view astronomical telescopes," *J. Opt. Soc. Am. A* **11**, 783–805 (1994).

[4] T. Fusco, J.-M. Conan, V. Michau, L.M. Mugnier, and G. Rousset, "Phase estimation for large field of view: application to multiconjugate adaptive optics," *SPIE* **3763**, 125–133 (1999).

[5] R. Flicker, B.L. Ellerbroek, and F.J. Rigaut, "Comparison of multiconjugate adaptive optics configurations and control algorithms for the Gemini-South 8m telescope," this volume.

[6] R. Ragazzoni, E. Marchetti, and G. Valente, "Adaptive-optics corrections available for the whole sky," *Nature* **403**, 54–56 (2000).

[7] F.J. Rigaut, M. Chun, M. Mountain, and R. Ragazzoni, "Adaptive Optics Challenges for the ELTs," Proc. ESO Workshop on Extremely Large Telescopes, in press (1999).

[8] E.P. Walner, "Optimal wave-front correction using slope measurements," *J. Opt. Soc. Am.* **73**, 1771–1776 (1983).

[9] B.M. Welsh and C.S. Gardner, "Effects of turbulence-induced anisoplanatism on the imaging performance of adaptive-astronomical telescopes using laser guide stars," *J. Opt. Soc. Am. A* **8**, 69–80 (1991).

[10] G.A. Tyler, "Merging: a new method for tomography through random media," *J. Opt. Soc. Am. A* **11**, 409–424 (1994).

[11] B.L. Ellerbroek and D.W. Tyler, "Modeling the combined effect of static and varying phase distortions on the performance of adaptive optical systems," *Appl. Opt.* **38**, 3857–3868 (1999).

[12] F. Riguat, em Report on the Seeing on Mauna Kea, (University of Hawaii, 1992).

[13] J. Vernin, A. Agabi, R. Avila, M. Azouit, R. Conan, F. Martin, E.Masciadri, L. Sanchez, and A. Ziad, *1998 Gemini Site Testing Campaign: Cerro Pachon and Cerro Tololo*, (Gemini Project, 2000).

Downloaded From: https://www.spiedigitallibrary.org/conference-proceedings-of-spie on 6/29/2018
Terms of Use: https://www.spiedigitallibrary.org/terms-of-use

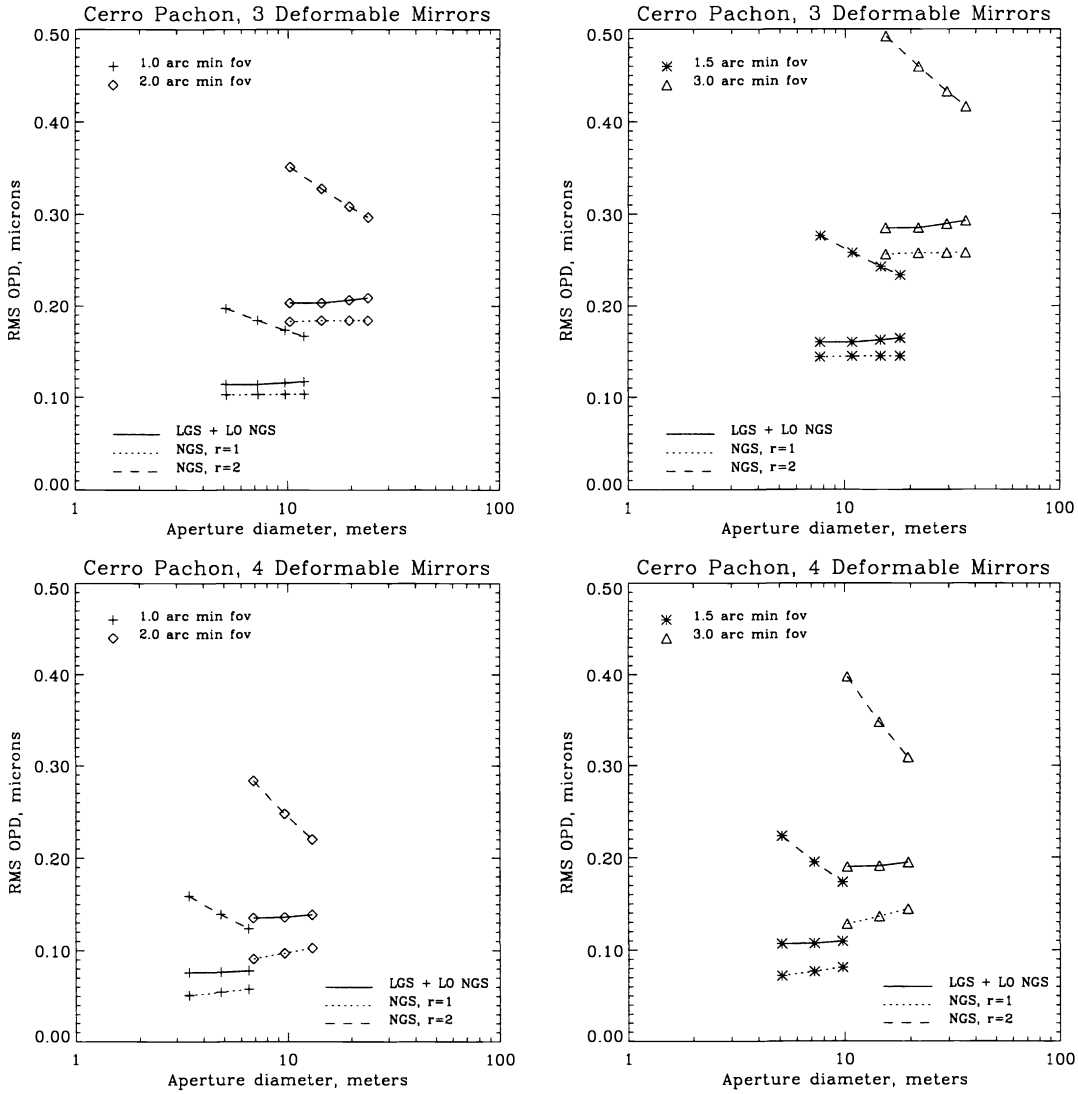

Figure 5: MCAO performance for the median Cerro Pachon turbulence profile

These results have been obtained by substituting specific aperture diameters and fields-of-views into the normalized results in Fig.'s 3 and 4. The field-of-view are specified in terms of their full widths (1, 1.5, 2, or 3 arc minutes).

Downloaded From: https://www.spiedigitallibrary.org/conference-proceedings-of-spie on 6/29/2018
Terms of Use: https://www.spiedigitallibrary.org/terms-of-use

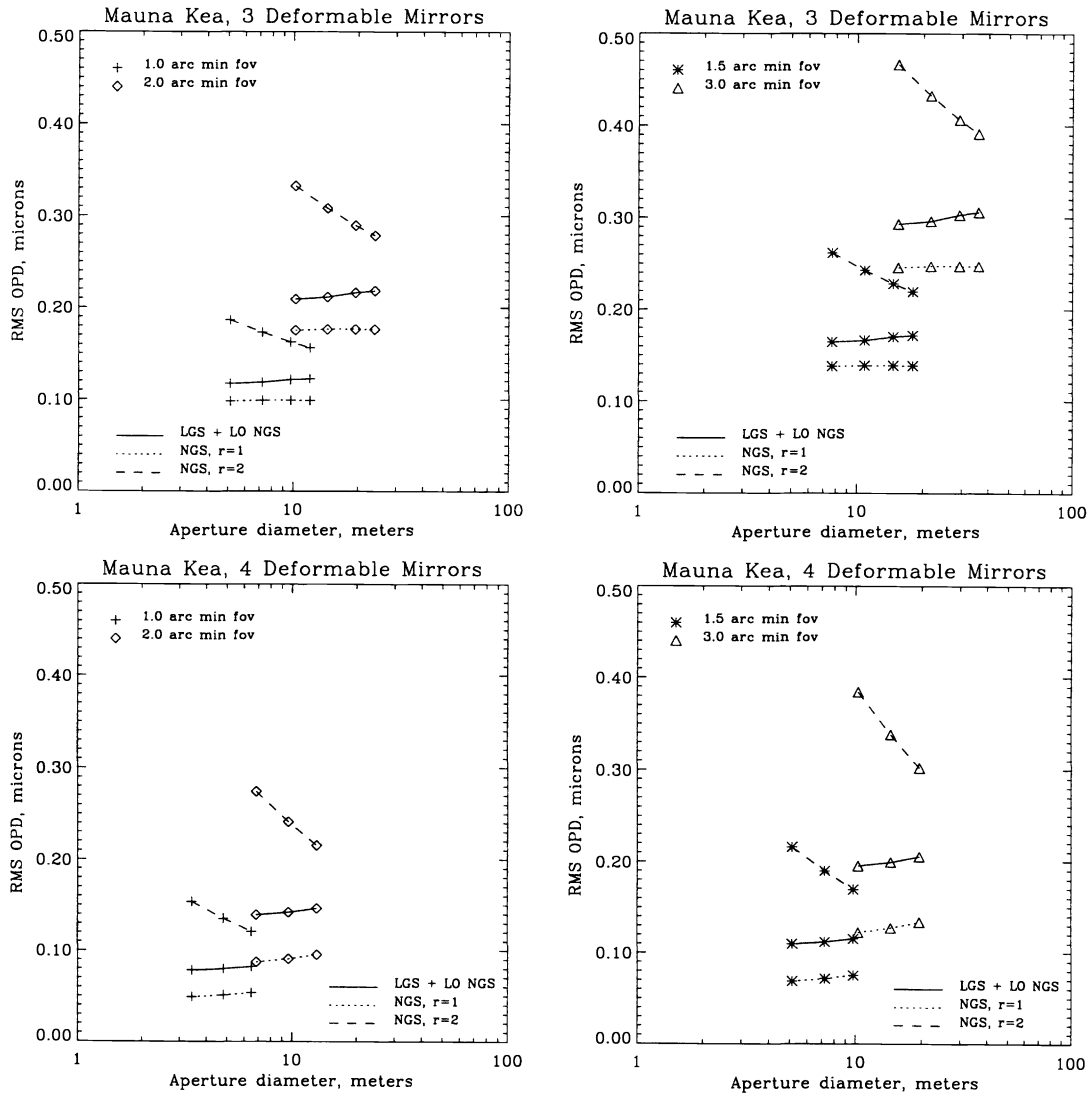

Figure 6: MCAO performance for the median Mauna Kea turbulence profile

These results are analogous to Fig. 5, except that they have been computed for the median Mauna Kea turbulence profile listed in Table 1.

Downloaded From: https://www.spiedigitallibrary.org/conference-proceedings-of-spie on 6/29/2018
Terms of Use: https://www.spiedigitallibrary.org/terms-of-use